Inorg. Chem. **2003**, *42*, 598–604

Synthesis, Structural and Spectroscopic Properties of Two New Ethylenediamine-Templated Gallophosphate–Oxalate Layered Materials

Maja Mrak,*,†,‡ Uwe Kolitsch,† Christian Lengauer,† Venčeslav Kaučič,‡ and Ekkehart Tillmanns†

Institut für Mineralogie und Kristallographie, Universität Wien, Geozentrum, Althanstrasse 14, A-1090 Vienna, Austria, and National Institute of Chemistry, Hajdrihova 19, SI-1000 Ljubljana, Slovenia

Received April 22, 2002

Two new layered gallophosphate–oxalate materials have been prepared hydrothermally using ethylenediamine and oxalic acid as structure-directing agents. The compounds $(C_2N_2H_{10})_2[Ga_2(C_2O_4)_2(HPO_4)_3]\cdot H_2O$ **1** and $(C_2N_2H_{10})_3[Ga_4(C_2O_4)_4(HPO_4)_4(H_2PO_4)_2]$ **2** are closely related, consisting of anionic double chains built of alternating pairs of GaO_6 and HPO_4 polyhedra. These double chains are linked via bridging HPO_4 or H_2PO_4 tetrahedra to form corrugated layers containing eight-membered rings. The oxalate group acts as a bidentate ligand to each of the GaO_6 octahedron. The corrugated layers are held together by strong to weak hydrogen-bonding interactions between oxalate groups, water and diprotonated ethylenediamine molecules, and the framework components. The compounds were characterized by single-crystal X-ray diffraction, thermogravimetric analysis, and infrared and Raman spectroscopy. Crystal data for **1**: monoclinic, space group $P2_1/c$ (No. 14), $a = 6.355(1)$ Å, $b = 39.362(8)$ Å, $c = 9.249(2)$ Å, $\beta = 106.7(1)°$, $Z = 2$. Crystal data for **2**: triclinic, space group $P\bar{1}$ (No. 2), $a = 8.730(1)$ Å, $b = 11.575(1)$ Å, $c = 11.696(1)$ Å, $\alpha = 115.12(1)°$, $\beta = 90.07(1)°$, $\gamma = 111.23(1)°$, $Z = 2$.

Introduction

The synthesis of novel open-framework organically templated metal phosphates under hydrothermal conditions represents a major activity in current solid-state chemistry. They are of scientific interest because of the challenges posed by their synthesis, processing, and characterization. Many of these materials are synthesized in the presence of organic amines as structure-directing agents, usually accommodated in the structural voids and not as a part of the skeleton. Recently, various reports have demonstrated that the phosphate groups can be either partially or completely replaced by multidentate carboxylates, resulting in open inorganic−organic hybrid materials. The underlying idea is to combine the robustness of inorganic frameworks with the flexibility of organic ligands. An interesting variant of the metal phosphates is obtained by incorporation of the oxalate group in the open frameworks. A number of metal phosphate−oxalates of Al, Fe, In, and Mn have been reported during the past two years.[1] In the framework of these compounds, the oxalate unit can act either as a ligand or as a bridging element. Very few, but intriguing, examples of gallium phosphate−oxalates have been reported to date. Two layered phosphate−oxalates built from GaO_4, GaO_6, PO_4, and oxalate units were reported: $[Ga_5(OH)_2(C_{10}H_9N_2)(C_2O_4)_2(PO_4)_4]\cdot 2H_2O$,[2] with GaO_4N polyhedra connecting the layers, and $(R\text{-}C_5H_{14}N_2)_2[Ga_4(C_2O_4)(H_2PO_4)_2(PO_4)_4]\cdot 2H_2O$,[3] with chiral *R*-2-methylpiperazinium cations located between the layers. Three-dimensional $K_2[Ga_4(C_2O_4)_2(PO_4)_4]\cdot 2H_2O$ with potassium cations and water molecules within the structural tunnels was characterized as a first phosphate−oxalate containing an alkali metal.[4]

In the present work, we report the synthesis, crystal structures, thermoanalytical behavior, and spectroscopic properties (FT-IR and Raman spectroscopy) of two new layered gallium phosphate−oxalates, $(C_2N_2H_{10})_2[Ga_2(C_2O_4)_2(HPO_4)_3]\cdot H_2O$ **1** and $(C_2N_2H_{10})_3[Ga_4(C_2O_4)_4(HPO_4)_4(H_2PO_4)_2]$ **2**.

* To whom correspondence should be addressed. E-mail: maja.mrak@ki.si.
† Universität Wien.
‡ National Institute of Chemistry.

(1) (a) Lethbridge, Z. A. D.; Tiwary, S. K.; Harrison, A.; Lightfoot, P. *J. Chem. Soc., Dalton Trans.* **2001**, 1904−1910. (b) Tsai, Y.-M.; Wang, S.-L.; Huang, C.-H.; Lii, K.-H. *Inorg. Chem.* **1999**, *38*, 4183−4187. (c) Chang, W.-J.; Lin, H.-M.; Lii, K.-H. *J. Solid State Chem.* **2001**, *157*, 233−239 and references therein.
(2) Chen, C.-Y.; Chu, P. P.; Lii, K.-H. *Chem. Commun.* **1999**, 1473−1474.
(3) Lii, K.-H.; Chen, C.-Y. *Inorg. Chem.* **2000**, *39*, 3374−3378.
(4) Hung, L.-C.; Kao, H.-M.; Lii, K.-H. *Chem. Mater.* **2000**, *12*, 2411−2417.

10.1021/ic025663r CCC: $25.00
Published on Web 12/24/2002

Experimental Section

Hydrothermal Synthesis. Compounds **1** and **2** were obtained by hydrothermal crystallization using gallium(III) oxide, phosphoric acid, ethylenediamine, boric acid, dihydrated oxalic acid, and distilled water. Ethylenediamine and oxalic acid were used as structure-directing agents. The relative molar composition of the reaction mixture was $0.5Ga_2O_3$, $2H_3PO_4$, 2ethylenediamine, $4H_3BO_3$, $2H_2C_2O_4{\cdot}2H_2O$, and $202H_2O$. Boric acid was used as an agent to promote the formation of the phosphate−oxalate structures.[5] In the synthesis procedure, four solutions were prepared: 4.92 g of phosphoric acid was dissolved in 46.1 mL of water, and each of the others (5.38 g oxalic acid, 5.28 g boric acid, and 2.56 g ethylenediamine) were dissolved in 10 mL of water. The solutions of oxalic acid, boric acid, and ethylenediamine were successively added to the solution containing the phosphoric acid and 2.00 g of finely dispersed gallium oxide. The suspension was thoroughly homogenized for 7 min using an ultrasonic mixer to generate a homogeneous mixture each time before the addition of the next component. After all the components were added, the gel was finally mixed for another 15 min. The resulting gel was transferred to Teflon-lined autoclaves and heated under static conditions at 165 °C in a furnace for 5 days, followed by cooling to room temperature with cold water. The crystallization products were washed with distilled water and dried at 80 °C. In the final product, there were two phases in the approximate ratio 1:1, bigger spherolitic aggregates of radiating colorless prisms **1** and smaller ones composed of whitish to colorless acicular crystals **2**. The spheroids were manually separated under an optical microscope. The compounds were then identified as **1** and **2** by powder X-ray diffraction (XRD) by comparison with the simulated XRD pattern from the single-crystal data. Separated powders were also prepared for thermal analysis and FT-IR spectroscopy.

Both phases were proven to be new compounds by X-ray powder diffraction data, recorded on a Philips X'PERT powder diffractometer with Ni-filtered Cu Kα radiation in the range 5−45° 2θ. The thermogravimetric analyses were performed using a computer-controlled (Mettler TG50) thermobalance under flowing air atmosphere (20 mL/ min) in the temperature range 30−1000 °C using a heating rate of 1 °C min^{-1}. The high-temperature X-ray powder diffraction data (24−350 °C) were collected on a Philips X'Pert MPD diffractometer in Debye−Scherrer geometry equipped with an in-house built capillary facility and a position-sensitive detector.

Crystallographic Structure Determination. Crystal structures of both compounds **1** and **2** were determined by single-crystal X-ray diffraction method at room temperature. Colorless prismatic crystals of dimension 0.05 × 0.11 × 0.13 mm^3 for **1** and 0.02 × 0.02 × 0.18 mm^3 for **2** were mounted on a Nonius Kappa CCD diffractometer equipped with a 0.3 mm diameter capillary-optics collimator to provide increased resolution. The experiment was carried out using graphite-monochromatized Mo Kα radiation (λ = 0.71073 Å) with a θ_{max} and crystal-to-detector distance of 27.50°, 42 mm for **1** and 26.37°, 30 mm for **2**. The data collections were performed by collecting 924 and 499 frames for **1** and **2**, respectively, with a total exposure time per frame of 500 s for **1** and 600 s for **2** (angular oscillation of 0.5° and 1° per frame for **1** and **2**, respectively). Measured intensity data were processed with the Nonius program suite DENZO-SMN and corrected for Lorentz, polarization, and absorption effects. The unit cell dimensions were determined by a least-squares fit of 9948 and 7350 reflections for **1** and **2**, respectively. Whole reciprocal spheres were collected up to $-8 \le h \le 8$, $-51 \le k \le 50$, $-12 \le l \le 11$ for **1**, and up to $-10 \le h \le 10$, $-14 \le k \le 14$, $-14 \le l \le 14$ for **2**. The numbers of measured and observed unique reflections with $I > 2\sigma(I)$ were 5082, 4555 for **1** and 4000, 2452 for **2.** On the basis of systematic absences and statistics of intensity distribution, the space group was determined to be $P2_1/c$ for **1** and $P\bar{1}$ for **2**. The first structure was solved by direct methods, and the second by Patterson methods (SHELXS-97),[6] followed by evaluation of subsequent difference Fourier maps. All non-hydrogen atoms were refined anisotropically. The refinement computations were performed with the SHELXL-97 program.[6] All of the hydrogen atoms in **1** were directly located from Fourier difference maps calculated at the final stage of structure refinements. For **2**, the H atoms could not be located, and slight orientational disorder was observed for P(3) and two of the three ethylenediamine molecules. The crystallographic data are summarized in Table 1. The final cycles of least-squares refinement converged at $R(F_o)$ = 0.0216 for **1** and 0.0566 for **2**. The final difference Fourier maps were characterized by $\Delta\rho_{max,min}$ = 0.41, −0.32 e $Å^{-3}$ for **1** and 0.96, −0.80 e $Å^{-3}$ for **2**. The values of the goodness-of-fit are 1.050 for **1** and 1.026 for **2**. The results of bond-valence calculations[7] were used to identify the hydroxo and water oxygen atoms.

Table 1. Crystallographic Data for **1** and **2**

	1	**2**
formula	$C_{16}H_{50}Ga_4N_8O_{42}P_6$	$C_7H_{19}Ga_2N_3O_{20}P_3$
fw	1491.34	697.60
Z	2	2
space group	$P2_1/c$ (No. 14)	$P\bar{1}$ (No. 2)
a, Å	6.355(1)	8.730(1)
b, Å	39.362(8)	11.575(1)
c, Å	9.249(2)	11.696(1)
α, deg	90	115.12(1)
β, deg	106.66(1)	90.07(1)
γ, deg	90	111.23(1)
V, $Å^3$	2216.5(7)	980.52(16)
D_{calcd}, $g{\cdot}cm^{-3}$	2.235	2.363
μ, mm^{-1}	2.761	3.107
T, °C	20	20
λ, Å	0.71073	0.71073
$R(F_o)^a$	0.0216	0.0566
$R_w(F_o^2)$	0.0528	0.1329

[a] $R(F_o) = \Sigma(||F_o| - |F_c||)/\Sigma|F_o|$; $R_w(F_o^2) = [\Sigma w(|F_o| - |F_c|)^2/\Sigma w|F_{o(2)}|]^{1/2}$.

IR and Raman Spectroscopy. FT-IR powder spectra were recorded in the 400−4000 cm^{-1} range on a Perkin-Elmer 1760X FT-IR spectrometer equipped with a TGS detector. Pressed KBr pellets were measured at a nominal resolution of 4 cm^{-1}. Single-crystal Raman spectra were collected on a Renishaw MicroRaman Imaging system (M1000) using excitation through a Leica DMLM optical microscope with a 488 nm Ar laser and a 633 nm He−Ne laser. Spectra were recorded between 100 and 4000 cm^{-1} with a spectral resolution of ±2 cm^{-1} and a minimum lateral resolution of ∼0.002 mm on the sample.

Results and Discussion

$(C_2N_2H_{10})_2[Ga(2)(C_2O_4)_2(HPO_4)_3]{\cdot}H_2O$. Compound **1** consists of corrugated anionic layers constructed from GaO_6 octahedra, HPO_4 tetrahedra, and planar oxalate groups, separated by ethylenediamine and water molecules (Figure

(5) Choudhury, A.; Natarajan, S.; Rao, C. N. R. *Chem. Mater.* **1999**, *11*, 2316−2318.

(6) Sheldrick, G. M. *SHELXS-97, a program for the solution of crystal structures. SHELXL-97, a program for crystal structure refinement*; University of Göttingen: Göttingen, Germany, 1997.

(7) Brown, I. D. *J. Appl. Crystallogr.* **1996,** *29*, 479−480.

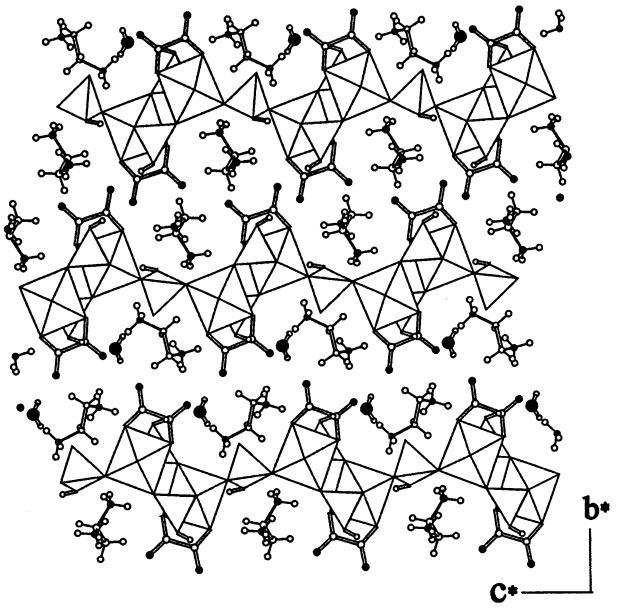

Figure 1. View of structure **1** along [100], showing a polyhedral representation of the anionic layers stacked along [010], with protonated ethylenediamine cations located between the layers. The water molecules (●) are situated in the space between adjacent layers.

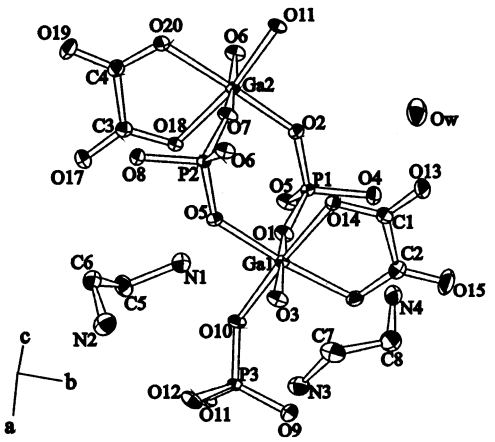

Figure 2. Perspective view of compound **1** showing the atom labeling scheme. Thermal ellipsoids are shown at 50% probability.

Table 2. Selected Bond Lengths (Å) for **1**

Ga(1)−O(5)	1.9335(13)	P(1)−O(3)	1.5197(14)
Ga(1)−O(10)	1.9515(13)	P(1)−O(2)	1.5146(14)
Ga(1)−O(3)	1.9576(13)	P(1)−O(1)	1.5114(14)
Ga(1)−O(1)	1.9689(13)	P(1)−O(4)	1.5829(15)
Ga(1)−O(14)	1.9871(13)	P(2)−O(5)	1.5114(14)
Ga(1)−O(16)	2.0113(14)	P(2)−O(6)	1.5147(14)
Ga(2)−O(2)	1.8892(13)	P(2)−O(7)	1.5282(14)
Ga(2)−O(11)	1.9392(13)	P(2)−O(8)	1.5810(15)
Ga(2)−O(6)	1.9399(13)	P(3)−O(9)	1.4976(14)
Ga(2)−O(7)	1.9937(13)	P(3)−O(10)	1.5263(14)
Ga(2)−O(18)	2.0021(13)	P(3)−O(11)	1.5308(14)
Ga(2)−O(20)	2.0402(14)	P(3)−O(12)	1.5969(15)

1). The asymmetric unit is shown in Figure 2, and selected bond lengths and angles are listed in Tables 2 and 3. There are two crystallographically nonequivalent gallium sites and three phosphorus sites. A single water molecule is located in the space between adjacent layers. The gallium coordination sphere consists of two oxalate oxygens and four phosphate oxygens. The oxalate anion acts as a bidentate

Table 3. Selected Bond Angles (deg) for **1**

O(5)−Ga(1)−O(10)	90.27(6)	O(2)−Ga(2)−O(11)	93.23(6)
O(5)−Ga(1)−O(3)	93.50(6)	O(2)−Ga(2)−O(6)	92.23(6)
O(10)−Ga(1)−O(3)	87.31(6)	O(11)−Ga(2)−O(6)	86.64(6)
O(5)−Ga(1)−O(1)	89.52(6)	O(2)−Ga(2)−O(7)	92.99(6)
O(10)−Ga(1)−O(1)	85.15(6)	O(11)−Ga(2)−O(7)	88.97(5)
O(1)−Ga(1)−O(3)	171.90(6)	O(6)−Ga(2)−O(7)	173.36(6)
O(5)−Ga(1)−O(14)	94.16(6)	O(2)−Ga(2)−O(18)	96.56(6)
O(10)−Ga(1)−O(14)	175.40(6)	O(11)−Ga(2)−O(18)	170.17(6)
O(3)−Ga(1)−O(14)	93.66(6)	O(6)−Ga(2)−O(18)	93.89(6)
O(1)−Ga(1)−O(14)	93.62(6)	O(7)−Ga(2)−O(18)	89.58(5)
O(5)−Ga(1)−O(16)	174.38(6)	O(2)−Ga(2)−O(20)	177.30(6)
O(10)−Ga(1)−O(16)	93.51(6)	O(11)−Ga(2)−O(20)	89.43(6)
O(3)−Ga(1)−O(16)	90.84(6)	O(6)−Ga(2)−O(20)	87.45(6)
O(1)−Ga(1)−O(16)	86.66(6)	O(7)−Ga(2)−O(20)	87.53(6)
O(14)−Ga(1)−O(16)	81.98(5)	O(18)−Ga(2)−O(20)	80.78(5)

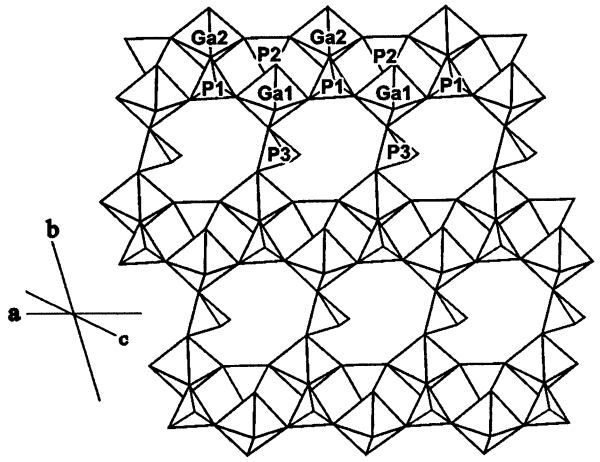

Figure 3. Projection of the structure of **1** perpendicular to the polyhedral anionic layers containing eight-membered rings.

ligand to the GaO_6 octahedra in a direction perpendicular to the plane of the layers. Thus, each octahedron is connected to four HPO_4 tetrahedra, while $HP(1)O_4$ and $HP(2)O_4$ tetrahedra are connected to three and $HP(3)O_4$ to two GaO_6 octahedra, respectively. Each layer (Figure 3) is constructed of double chains along (010) consisting of $Ga(1)O_6$ and $Ga(2)O_6$ octahedra, coordinated via $HP(1)O_4$ and $HP(2)O_4$ tetrahedra. These double chains are linked via bridging $HP(3)O_4$ tetrahedra to form an anionic layer parallel to (010). The polyhedral linkage within the layer units leads to the formation of unoccupied eight-membered rings constructed of alternating GaO_6 octahedra and HPO_4 tetrahedra. The layers are similar to those in compound **2**, $(R\text{-}C_5H_{14}N_2)_2[Ga_4(C_2O_4)(H_2PO_4)_2(PO_4)_4]\cdot 2H_2O$,[3] and $(C_2N_2H_{10})_{2.5}[Al_4(C_2O_4)_4(HPO_4)_4(H_2PO_4)_2]$.[8] The slight distortion observed for both GaO_6 octahedra is due to the attached oxalate groups, as indicated by the wide range of Ga−O bond lengths [1.934(1)−2.011(1) Å for Ga(1) and 1.889(1)−2.040(1) Å for Ga(2)] and the narrow O−Ga−O angles [81.98(5)−94.16(6)° for Ga(1) and 86.64(6)−96.56(6)° for Ga(2)], similar to distortions observed in other metal phosphate−oxalates. The HPO_4^{2-} anions have two or three oxygens coordinated to gallium, with bond lengths typical of those found previously in other gallophosphate materials. One of the four P−O bonds of each HPO_4 group is considerably longer [P(1)−

(8) Lightfoot, P.; Lethbridge, Z. A. D.; Morris, R. E.; Wragg, D. S.; Wright, P. A.; Kvick, Å.; Vaughan, G. B. M. *J. Solid State Chem.* **1999**, *143*, 74−76.

Table 4. Hydrogen Bonds in **1**

D−H···A	*d*(D···A)	∠DHA	*d*(H···A)
O(4)−H(21)···OW	2.609(2)	172(3)	1.885(19)
O(8)−H(22)···O(19)	2.697(2)	179(3)	1.957(19)
O(12)−H(23)···O(7)	2.602(2)	158(3)	1.90(2)
OW−HW1···O(9)	2.899(2)	156(3)	2.16(2)
OW−HW2···O(15)	2.732(2)	165(3)	1.96(2)
N(1)−H(5)···O(10)	2.899(2)	175(3)	2.007(13)
N(1)−H(6)···O(18)	2.908(2)	171(3)	2.016(14)
N(1)−H(7)···O(12)	2.858(2)	152(3)	2.029(18)
N(2)−H(8)···O(17)	2.801(3)	165(3)	1.912(15)
N(2)−H(9)···O(10)	3.145(3)	137(2)	2.42(2)
N(2)−H(10)···O(20)	2.832(3)	166(3)	1.942(14)
N(3)−H(15)···O(13)	2.835(3)	155(3)	2.005(17)
N(3)−H(16)···O(11)	3.020(2)	153(3)	2.198(17)
N(3)−H(17)···O(9)	2.813(2)	160(3)	1.955(15)
N(4)−H(18)···O(9)	2.851(2)	164(3)	1.986(15)
N(4)−H(19)···O(13)	2.803(2)	160(3)	1.948(15)
N(4)−H(20)···O(4)	3.133(3)	171(3)	2.254(13)

O(4), P(2)−O(8), and P(3)−O(12)] than the remaining bonds, which is consistent with the presence of distinct P−OH groups. The P(3)−O(9) bond is significantly shorter with a distance of 1.498(1) Å, implying that this bond has some double bond character. This assignment is supported by the location of hydrogens in difference Fourier maps and by bond-valence calculations.[7] There is a complex network of hydrogen bonds within each layer (Table 4) but no direct hydrogen bonds between adjacent layers. The protonated ethylenediamine molecules and the single water molecule are sandwiched between the layers. Like in most organic−inorganic solid compounds, organic amines exist as charge-balancing cations in the diprotonated state and serve as H-bond donors to the nearest framework oxygen. The cohesion of the structure is mainly ensured through the interaction of the NH_3^+ terminal groups of the ethylenediamine and the oxygen atoms of the oxalate groups as well as of bridging Ga−O−P oxygens, with N···O distances in the range 2.801(3)−3.145(3) Å (Table 4). The strongest hydrogen-bond interactions occur between the OH group of the HPO_4 tetrahedra and, as acceptors, the water molecule, a bridging framework oxygen atom, and an oxalate oxygen (O···O distances from 2.602(2) to 2.697(2) Å). Furthermore, the water molecule participates in a strong hydrogen bond with an oxalate oxygen (Ow···O(15): 2.732(2) Å).

$(C_2N_2H_{10})_3[Ga_4(C_2O_4)_4(HPO_4)_4(H_2PO_4)_2]$ (2). The crystal structure of **2** consists of corrugated anionic $[Ga_4(C_2O_4)_4(HPO_4)_4(H_2PO_4)_2]^{6-}$ layers, oriented approximately parallel to the $(0\bar{1}1)$ plane, with charge-balancing $[NH_3CH_2CH_2NH_3]^{2+}$ cations located between and, in contrast to **1**, within the layers (Figure 4). The asymmetric unit is shown in Figure 5. Selected bond lengths and angles are given in Tables 5 and 6, respectively. Compound **2** displays a connectivity similar to that in **1**. Again, there are double chains, but within each chain, both HP(1,2)O_4 tetrahedra as well as Ga(1,2)O_6 octahedra are connected in an alternating manner along each single chain (Figure 6). As in **1**, the double chains are linked to each other via the H_2PO_4 group to form corrugated layers again containing eight-membered rings. However, by comparison to **1**, the structure contains no water molecule. Two ethylenediamine molecules (with N(1) and N(3)) are located in the space between the layers, the third one (N(2)) passes through the eight-membered ring and is orientationally disordered. Modeling of the disorder of the latter yielded refined site occupancies of 0.876(11), 0.063(4), and 0.062(10) for N(2A), N(2B), and N(2C), which represent alternate positions of N(2); the site occupancies of the alternate positions of the other disordered ethylenediamine molecule were too low to be modeled. The P(3) atom of the $H_2P(3)O_4$ group was found to be disordered over two positions (P(3A)−P(3B): distance 1.44(2) Å) with refined site oc-

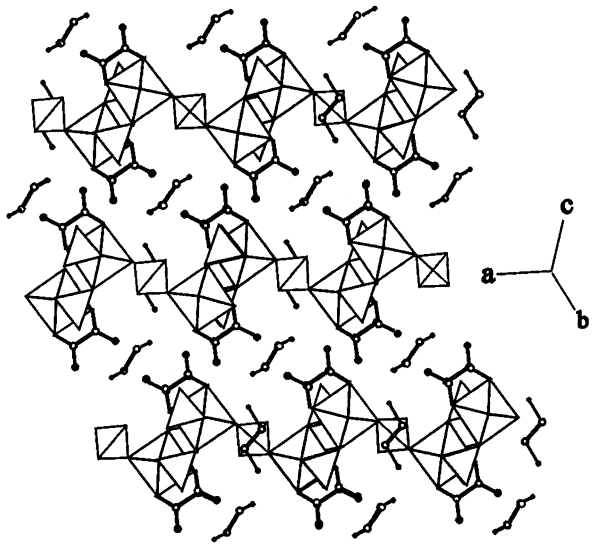

Figure 4. View of the structure of **2** showing a polyhedral representation of the corrugated anionic layers approximately parallel to $(0\bar{1}1)$, with protonated ethylenediamine cations located between the layers.

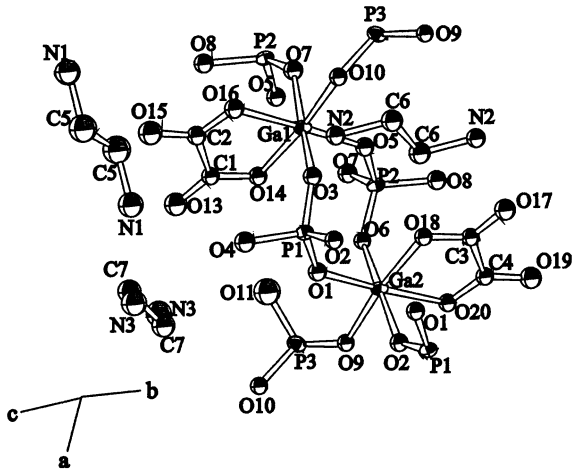

Figure 5. Atoms of the asymmetric unit of **2** showing the atom labeling scheme and thermal ellipsoids at 50% probability.

Table 5. Selected Bond Lengths (Å) for **2**

Ga(1)−O(5)	1.895(5)	P(1)−O1	1.505(5)
Ga(1)−O(3)	1.918(5)	P(1)−O(2)	1.524(5)
Ga(1)−O(7)	1.951(5)	P(1)−O(3)	1.523(5)
Ga(1)−O(10)	1.977(4)	P(1)−O(4)	1.576(5)
Ga(1)−O(14)	1.985(4)	P(2)−O(5)	1.515(5)
Ga(1)−O(16)	2.003(5)	P(2)−O(7)	1.523(5)
Ga(2)−O(1)	1.908(5)	P(2)−O(6)	1.527(4)
Ga(2)−O(2)	1.922(4)	P(2)−O(8)	1.586(5)
Ga(2)−O(6)	1.948(4)	P(3A)−O(9)	1.494(5)
Ga(2)−O(9)	1.956(4)	P(3A)−O(10)	1.504(5)
Ga(2)−O(18)	1.992(4)	P(3A)−O(12)	1.566(6)
Ga(2)−O(20)	2.044(5)	P(3A)−O(11)	1.570(6)

Table 6. Selected Angles (deg) for **2**

O(5)−Ga(1)−O(3)	93.4(2)	O(1)−Ga(2)−O(2)	94.35(19)
O(5)−Ga(1)−O(7)	90.2(2)	O(1)−Ga(2)−O(6)	91.77(19)
O(3)−Ga(1)−O(7)	172.1(2)	O(2)−Ga(2)−O(6)	171.5(2)
O(5)−Ga(1)−O(10)	93.33(19)	O(1)−Ga(2)−O(9)	93.54(19)
O(3)−Ga(1)−O(10)	86.01(18)	O(2)−Ga(2)−O(9)	86.49(18)
O(7)−Ga(1)−O(10)	86.80(19)	O(6)−Ga(2)−O(9)	87.24(18)
O(10)−Ga(1)−O(14)	172.15(19)	O(1)−Ga(2)−O(18)	95.04(19)
O(5)−Ga(1)−O(16)	176.38(19)	O(2)−Ga(2)−O(18)	91.90(19)
O(3)−Ga(1)−O(16)	88.24(19)	O(6)−Ga(2)−O(18)	93.45(18)
O(7)−Ga(1)−O(16)	88.6(2)	O(9)−Ga(2)−O(18)	171.37(19)
O(10)−Ga(1)−O(16)	90.01(19)	O(1)−Ga(2)−O(20)	176.70(18)
O(14)−Ga(1)−O(16)	82.21(19)	O(2)−Ga(2)−O(20)	86.72(19)
O(5)−Ga(1)−O(14)	94.5(2)	O(6)−Ga(2)−O(20)	87.50(19)
O(3)−Ga(1)−O(14)	92.67(19)	O(9)−Ga(2)−O(20)	89.64(18)
O(7)−Ga(1)−O(14)	94.01(19)	O18−Ga(2)−O(20)	81.80(18)

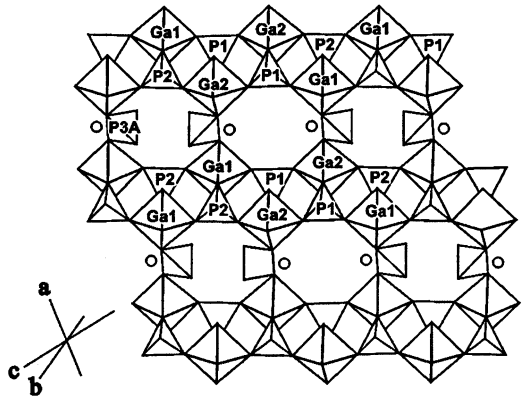

Figure 6. Projection of the gallophosphate−oxalate layer in **2** with four and two types of eight-membered rings (one with $H_2P(3)O_4$ tetrahedra pointing inward and the other pointing outward). Note that the $H_2P(3)O_4$ groups are statistically disordered over two orientations (P(3A) in the center of the $P(3A)O_4$ tetrahedra, P(3B) shown as small sphere).

Table 7. Probable Hydrogen Bond Interactions in **2**

D···A	*d*(D···A)	D···A	*d*(D···A)
O(4)···O(15)	2.596(7)	N(2B)[a]···O(9)	2.35(1)
O(8)···O(19)	2.591(7)	N(2B)[a]···O(10)	2.46(9)
O(11)···O(1)	2.985(7)	N(2B)[a] ···O(5)	2.91(9)
O(11) ···O(6)	2.786(7)	N(2B)[a]···O(3)	3.06(9)
O(12)···O(5)	2.929(7)	N(2C)[a]···O(10)	2.49(9)
O(12) ···O(7)	2.824(7)	N(2C)[a]···O(9)	2.40(9)
O(12)···O(14)	3.010(7)	N(2C)[a]···O(1)	3.01(9)
N(2A)[a]···O(2)	2.852(8)	N(2C)[a]···O(2)	2.85(9)
N(2A)[a]···O(3)	2.905(8)		

[a] Partially occupied site of alternate orientation of N(2) in orientationally disordered ethylenediamine molecule

cupancies of 0.911(3) and 0.089(3), respectively. Because of the main $H_2P(3)O_4$ tetrahedral orientations, half of the eight-membered rings have the OH groups of the $H_2P(3)O_4$ groups pointing toward the center of the ring and do not contain the ethylenediamine molecules, whereas the other half contain them (see Figure 6). If one now considers the orientation of the disordered $H_2P(3)O_4$ group and of the disordered ethylenediamine molecule passing through the ring, one can correlate the position of the P(3)−OH hydroxyl groups with the template orientation. It is likely that the correlated disorder is dictated by strong hydrogen bonding between the involved units (see Table 7). A similar disorder was observed in monoclinic $(C_2N_2H_{10})_{2.5}[Al_4H(C_2O_4)_4(HPO_4)_4(H_2PO_4)_2]$,[8] which also shows a topology almost identical to that of **2**. A comparably correlated disorder, involving an aza-crown ether as a structural agent and HPO_4 groups, has been reported in the oxyfluorinated compound MIL-1.[9]

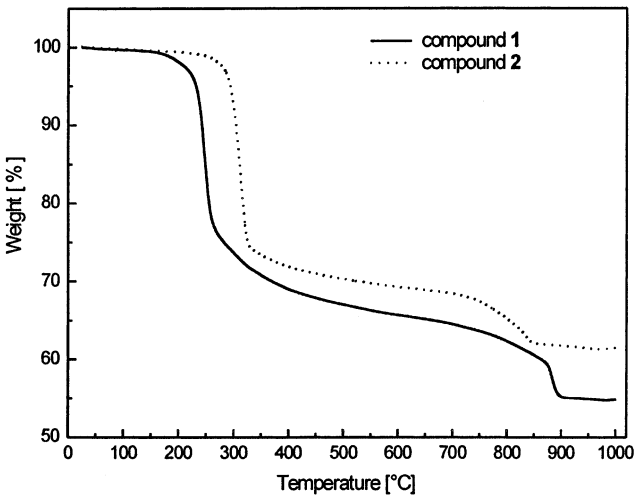

Figure 7. TGA curves for **1** and **2** in flowing air at 1 °C min^{-1}.

Bond-valence calculations show that the four phosphate oxygens O(4), O(8), O(11), and O(12) have valence sums of 1.38, 1.35, 1.40, and 1.42, respectively, and all other oxygen atoms have values close to 2, thus indicating, along with the refined P−O bond lengths, that O(4), O(8), O(11), and O(12) are hydroxo oxygens. The hydroxyl groups are donors of strong hydrogen bonds to oxalate oxygens and weak ones to framework oxygens, as listed in Table 7 (left column).

Thermogravimetric Analysis. The TG curves of both compounds (Figure 7) can be split up into two steps, although these are not well separated. Compound **1** shows a total weight loss of 45.1%, which starts with a first step at ca. 200 °C followed by a weak gradual weight decrease up to ∼750 °C. This first mass loss can be attributed to the removal of the one molecule of water and three ethylenediamine molecules and the decomposition of two oxalate groups per formula unit (calcd 38.3%). The decomposition of the oxalate probably leads to the formation of a mixture of 2CO and $2CO_2$, also observed for many other metal oxalates. Between ∼760 and 930 °C, a second, broad step (∼6.8%) is recorded, which is attributed to the loss of the three hydroxyl groups. The observed total weight loss (45.1%) is in very good agreement with the calculated value of 45.1%. A similar weight loss profile is obtained for compound **2** (observed 39.3%), with the first step starting at ca. 260 °C, followed again by a weak gradual weight decrease up to ∼750 °C. This is attributed to the loss of three ethylenediamine molecules and decomposition of four oxalate groups to a mixture of 8CO and $8CO_2$ (calcd 33.9%). Above ∼750 °C, a second step (7.5%) occurs which can be attributed to the partial decomposition of eight hydroxyl groups (calcd ∼9.7%). The agreement between measured and calculated total weight loss is less good than for compound **1**, tentatively explained by the incomplete decomposition of the hydroxyl groups.

(9) Serpaggi, F.; Loiseau, T.; Taulelle, F.; Ferey, G. *Microporous Mesoporous Mater.* **1998**, *20*, 197−206.

Table 8. IR and Raman Spectra of Compounds **1** and **2**

	IR/cm^{-1}	Raman/cm^{-1}	IR/cm^{-1}	Raman/cm^{-1}
Ga−O	ν_s 1152 vs	ν_s 1078 s	ν_s 1127 sh	ν_s 1058 sh,
	ν_s 1062 vs	ν_s 600 s	ν_s 1059 s	ν_s 599 m
	ν_s 600 s	ν 388 s	ν_{as} 556 m	
		HPO_4^{2-}		
P−OH	δ 1458 sh	δ 1461 m	δ 1476 s	δ 1464 vs
	ν_{as} 1101 vs	ν_{as} 1058 w	νas 1109 vs	ν_{as} 1130 sh
	ν_{as} 1042 sh		ν_{as} 1039 vs	ν_{as} 1041 vs
	ν_s 668 m		ν_s ca. 669 m	
δ O−P−O	ca. 556 sh	553 s	556 vs	557 s
	465 sh	480 s	ca. 465 sh	464 s
$H_2PO_4^-$			ν 874 s	
oxalate group	ν_{as} 1692 vs	ν_{as} 1692 vs	ν_{as} 1686 vs	ν_{as} 1702 m
O−C−O	ν_s 1325 sh	ν_s 1352 m	ν_s 1340 sh	ν_s 1345m
	ν_s 1291 m		ν_s 1315 s	
C−O	ν_s 1434 s	νs 1444 vs	νs 1429 s	ν_s 1466 s
	ν_{as} 819 w	ν_{as} 823 s	ν_{as} 795 s	ν_{as} 766 vw
δ C−O + δ O−C=O	794 s, 474 s	480 s	790 sh, 500 s	464 s
		Ethylenediamine		
ν OH_2 + NH_3^+ + CH_2	3500−2850	3040−2830	3500−2800	3540−2840
	1400−1200	1400−1200	1400−1200	1400−1200
δ OH_2 + δ NH_3^+	1611 sh	1615 s	1617 sh	1620 m
ρ NH_3^+ + ν C−C	908 s	910 vs	914 vs	914 sh

A similar weight loss profile is obtained for compound **2** (obsd 39.3%), with the first step starting at ca. 260 °C, followed again by a weak gradual weight decrease up to ∼750 °C. This is attributed to the loss of three ethylenediamine molecules and the decomposition of four oxalate groups to a mixture of 8CO and 8CO_2 (calcd 33.9%). Above ∼750 °C, a second step (7.5%) occurs which can be attributed to the partial decomposition of the eight hydroxyl groups (calcd 9.7%). The agreement between measured and calculated total weight loss is less good than that for compound **1**, tentatively explained by the incomplete decomposition of the hydroxyl groups.

The thermal stability of both compounds was studied by high-temperature X-ray powder diffraction (HT-XRD). During the heating, no significant changes in the powder patterns were observed from room temperature up to 250 °C (measured in steps of 50 °C). Between 250 and 300 °C, both structures collapse into an amorphous phase. The X-ray powder diffraction patterns of the residues of the thermogravimetric analysis and the HT-XRD measurements correspond to a mixture of major $GaPO_4$ (ICDD-PDF 31-0546) and very minor Ga_2O_3 (ICDD-PDF 43-1012).

Spectroscopic Studies. The powder infrared and single-crystal Raman spectra of compound **1** and **2** are shown in Figures 8 and 9, respectively. The complex IR spectra of both compounds show strong and broad bands in the 3500−2800 cm^{-1} range assignable to ν(OH) and ν(NH) bands in agreement with the participation of water molecules and ethylenediammonium cations in a weak to strong hydrogen bonding.[10] According to several spectroscopic studies on inorganic oxalates and metallic phosphates with ethylenediammonium cations, some of the observed bands can be assigned to the vibration of ethylenediammonium cations,

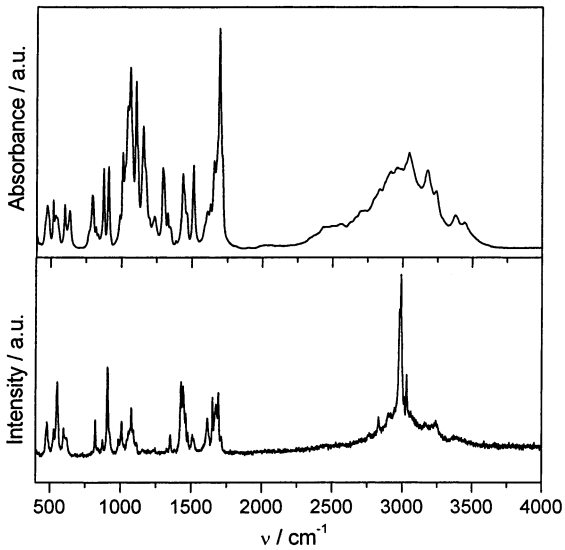

Figure 8. IR (top) and Raman spectra (bottom) of **1**.

chelating oxalato, gallium oxygen bonds,[11] and hydrogen phosphate anions (Table 8).[12] The ethylenediammonium cation bands are found in the ranges characteristic of the stretching vibrations of N−H and C−H bonds, as well as bending modes of the −CH_2− groups between 3500−2800

(10) (a) Armentano, D.; Munno, G.; Faus, J.; Lloret, F.; Julve, M. *Inorg. Chem.* **2001**, *40*, 655−660. (b) Chen, X.-F.; Cheng, P.; Liu, X.; Zhao, B.; Liao, D.-Z.; Yan, S.-P.; Jiang, Z.-H. *Inorg. Chem.* **2001**, *40*, 2652−2659.

(11) (a) Bollo, I. L.; Baran, E. J.; Garcia, A. C. *J. Therm. Anal.* **1986**, *31*, 1301−1308. (b) Farmer, V. C. *The infrared spectra of minerals*; Mineralogical Society: London, 1974.

(12) (a) Escobal, J.; Pizarro, J. L.; Mesa, J. L.; Lezama, L.; Olazcuaga, R.; Arriortua, M. I.; Rojo, T. *Chem. Mater.* **2000**, *12*, 376−382. (b) Do, J.; Bontchev, R. P.; Jacobson, A. J. *Inorg. Chem.* **2000**, *39*, 3230−3237. (b) Escobal, J.; Pizzaro, J. L.; Mesa, J. L.; Lezama, L.; Olazcuaga, R.; Arriortua, M. I.; Rojo, T. *Chem. Mater.* **2000**, *12*, 376−382.

(13) (a) Gharbi, A.; Jouini, A.; Averbuch-Pouchot, M. T.; Durif, A. *J. Solid State Chem.* **1994**, *111*, 330−337. (b) Kamoun, S.; Jouini, A.; Daoud, A. *J. Solid State Chem.* **1992**, *99*, 18−28.

(14) (a) Nakamoto, K. *Infrared and Raman Spectra of Inorganic and Coordination Compounds*; John Wiley & Sons: New York, 1997. (b) Martin, L.; Turner, S. S.; Day, P.; Guionneau, P.; Howard, J. A. K.; Hibbs, D. E.; Light, M. E.; Hursthouse, M. B.; Uruichi, M.; Yakushi, K. *Inorg. Chem.* **2001**, *40*, 1363−1371. (c) Do, J.; Bontchev, R. P.; Jacobson, A. J. *Chem. Mater.* **2001**, *13*, 2601−2607.

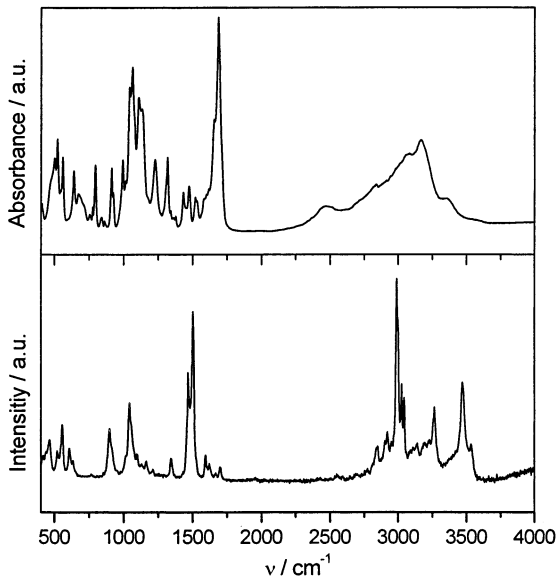

Figure 9. IR (top) and Raman spectra (bottom) of **2**.

cm^{-1} and 1400−1200 cm^{-1}.[13] The oxalate group vibrations $\nu_{as}(COO^-)$, ν_s (COO^-), $\nu(C-O)$, and $\delta(COO^-)$ are similar to those observed in other bichelating oxygen-donor oxalates,[14] and this is in agreement with the result of the X-ray analysis. The major differences between those two structures are confirmed by additional characteristic bands present only in one of them. First, there are characteristic bands at 3445 and 3377 cm^{-1} due to the ν(OH) stretching vibrations of lattice water molecules present only in **1**, whereas there is an additional band at 874 cm^{-1} in **2** corresponding to the P−OH stretching vibrations of the dihydrogen phosphate group.[11] The Raman spectra are equally complex and less similar to each other than the IR spectra, especially in the region above 3000 cm^{-1}. It is noteworthy that compound **2**, unlike **1**, exhibits two more very strong bands around 3470 and at 3262 cm^{-1}. We could ascribe this to the additional O−H hydrogen bonding involving the disordered dihydrogen phosphate group present in compound **2** (see Table 5).

Acknowledgment. We thank Dr. Dietmar Voll and Dr. Michael Andrut for helping with IR measurements. This research has been supported by a Marie Curie Fellowship of the European Community program 1.4.1 IHP under Contract HPMT-CT-2000-00138.

Supporting Information Available: Listing of X-ray crystallographic data in CIF format for the structure determination of **1** and **2**. This material is available free of charge via the Internet at http://pubs.acs.org.

IC025663R